2023 The 23rd International Conference on Control, Automation and Systems (ICCAS 2023)
Yeosu Venezia Hotel & Utop Marina Hotel, Yeosu, Korea, Oct. 17~20, 2023

Modelling and Design a Self-balancing Dual-wheeled Robot with PID Control

Santiago Nougues[1], Santiago Melo Guayacan[1], Daniela Garzón Cuadros[1],
Hernando Leon-Rodriguez.

Industrial Engineering Department; Nueva Granada Military University, Bogota – Colombia.
(est.santiago melo1@unimilitar.edu.co, est.santiago nougues@unimilitar.edu.co, est.daniela.garzon@unimilitar.edu.co,
hernando.leon@unimilitar.edu.co*)

Abstract: This article presents the design and control of a Segway robot based in a dual-wheeled platform that is kept in balance based on the inverted pendulum system; this has 2 points of balance: the bottom gives stability to the robot and the top is the unstable part. The goal of the platform is intended to stay upright; for doing so, the electronics components are placed on top in order to generate the signals from the controller & sensors to the motors. It was developed by means of an Arduino controller, in conjunction with an accelerometer and gyroscope to estimate and obtain the angle of inclination to make the determine motion of the robot. It works through cell phone apps with a Bluetooth and Wi-Fi connection. On the other hand, the paper presents the physical and mathematical theory for support its operation.

Keywords: Self-balancing, control design, Segway robot, dual-wheeled robot, PID control.

1. INTRODUCTION

Over the years, robots are becoming more and more important in human life, in most cases to improve or help the activities of industry, exploration, testing or even leisure. Currently, it has been developing technology related to transportation, such as the Segway which consists of modelling a robot with a PID controller and thus be able to have a 2-wheeled robot [1], in this case the rocker robot is considered a mobile robot, this has the quality of being able to balance on its two wheels without falling, due to an inverted pendulum system; however, this system is quite unstable compared to other types of robots. As regards, it was developed in such a way as to generate the least possible instability.

The robot has advantages that distinguish it from other robots, for example, it is evident that it is a robot with a small size, versatile, easy to transport, and it is possible to build with a low investment capital. Due to its inverted pendulum system, it has unstable, complicated multivariable and nonlinear properties [1].

In the development of the article will be mentioned the systems by which the robot works one of them is by means of two systems the inverted pendulum and the other, is to provide energy to the robot was connected to direct current that generates a force/torque relationship to be able to maintain the position in vertical. Also, use will be made of dynamic equations of motion.

In December 2001, the first innovative 2-wheel Segway robot for human transportation was presented. Thanks to its speed and versatility, it is considered as a transport for short distances, it is a product that revolutionized the market; in addition, it presents a system of operation by means of self-balancing and occupies little space. In 2003, the robot had some structural changes, such as changing the control system, which sends orders, by a communication system through a computer that had an integrated control platform, thus seeking to make the Segway work in all environments [2]. However, to reach a result, years of studies were needed, because at the beginning the robot did not transport humans, it was only balanced with its weight, the challenge of the engineers was to make the robot work with a person driving it, a positioning system was developed, where the displacement is measured, from the beginning, it resembles the estimation of the distance thanks to the rotation of the wheels and adding multiple sensors. [3]. Now powerful Segway also designed with capability of transport injured athletes based that current process is unstable for the player and ergonomically irresponsible for the medical personnel [4].

There are a great variety of Segway robots, three in particular will be mentioned: the first, its operation is based on an infrared proximity sensor, this allows to calculate the distance that the sensor is from the ground, the light bounces in the direction of the receiver to send the signal, that it has to be rebalanced, the second the most popular, which was developed the robot of this article, a sensor that has integrated an accelerometer and a gyroscope, Its function is based on the degrees of inclination according to its direction and movement of the robot [5] and the third is an autonomous robot developed at the University of Australia, using a LQR controller to obtain the appropriate force that the robot needs to stand, in addition to implementing the Kalman filter and thanks to this successfully eliminated the gyroscope, increasing the effectiveness of the angle of inclination; is designed to help elderly people to move around in wheelchairs[1].

Figure 1 shows the Cassie biped robot presented by the University of Michigan, Caltech and Harvard University

[1] All authors have contributed equally

at the end of August that works with the theory of the inverted pendulum, also must consider the movement of the legs, the weight of the same, stabilization of the step, the conditions of the motor, the states of movement, etc. Also, the controller allows the robot to keep me standing, walking towards all directions and in all environments. This type of robots are usually designed for search and rescue, since, they have a faster arrival than a human being and consume little energy [6].

Another range of robots that work with self-balancing are the omnidirectional robots designed to operate in any environment, however, these robots are much more complex to handle and perform, since it is necessary to consider aspects such as: the trajectory, the type of environment, possible restrictions, reaction time, the point of equilibrium in the environment, among others. They are robots that require a lot of computational work when establishing all the control and operation, with respect to the trajectories of passage, direction and inclination [19]. Actually, researches have expanded the applications of hybrid system of wheel-legged robot with enormous capabilities and locomotion [20] [21].

Several studies have shown constant short comings in the robots with respect to the energy they use, because the batteries they use regularly do not support the entire operation and negatively affect the use of the robot [22]. Finally some other studies are including in the virtual environment within parallel platforms [23].

Fig. 1. The first image shows Cassie, the next robot with sporting characteristics, and the last two shows a Segway transport robot [6].

2. MECHANICAL DESIGN

The weight of the robot and its center of gravity is distributed mostly in the lower part of the platform [7], where the motors are located, as shown in the figure 1; this helps to generate a better stability. Additionally, for the electronic assembly, it was considered that the robot is made of a metallic material, for such reason, at the time of organizing the components; an insulating plate was placed so as not to generate any type of reaction in the robot. The motors were soldered with wires to be connected to the H-bridge.

Table 1 show the measurements of the self-balancing robot, which was designed in such a way that when assembling all the electronic parts it remains in balance.

Figure 2 shows the conceptual robot built by metallic and plastic materials; this also influences its operation, so it must always be considered at the time of design.

Table 1. Structural characteristics of self-balancing

Characteristics	***Size***
Weight	*800 g*
Distance between wheels	*20.8 cm*
Length from middle bar to top bar	*5 cm*
Wheel diameter	*10 cm*
Width of each wheel	*2.5 cm*

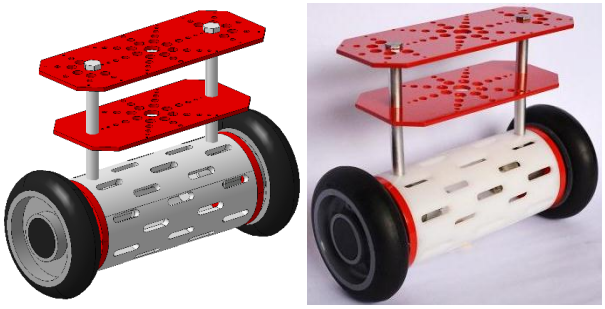

Fig. 2. Conceptual design of a dual-wheeled robot.

3. CONTROL SYSTEM

The control module consists of the Arduino Uno, which is responsible for executing the digital monitoring algorithm; it also receives the sensor signal from the sensing module and compares it with the position signal of the self-balancing. Digital PID algorithms are activated and thereby generate the control signals to balance the robot.

The actuation module sends signals to deliver the power to be able to move the motors that are coupled to the wheels that allow balancing the system [8]. In this case, the H-bridge was used as a driver whose function is to send control signals from the control module to power the motors. In this way, the communication module transmits through signals to the application in order to move the robot.

The Proportional-Integral-Derivative (PID) control allows to adequately controlling the robot, since it is the one that allows directing the signals on the position of the robot [9]. In this case the equilibrium is at an angle of 180 degrees, then the proportional value acts in such a way that at the end it stabilizes and reaches the goal of 180.

The most important element is the inertial measurement unit (IMU) works by means of the MPU sensor; it combines a gyroscope and an accelerometer on the same chip. It is configured in such a way that, when it moves forward, it tilts 1° forward and backward, i.e., when the movement is forward, it moves at 181° and conversely, it will have an angle of 179°. It also has a built-in 3.3 V voltage regulator. In the prototype it is as follows:

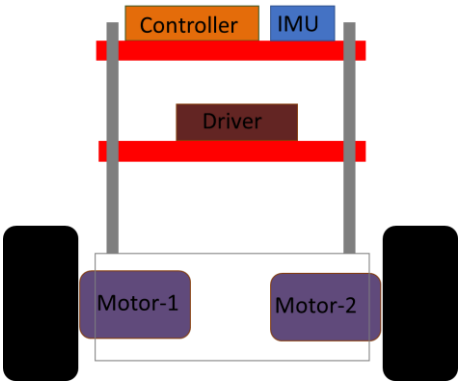

Fig. 3. Self-balancing distribution of components.

The gyroscope allows to know the angle in time, while it is moving or rotating with an angular velocity, thus being able to determine the behaviour that the robot is having. With respect to the accelerometer, it indicates the acceleration that occurs when there is movement along the axis, it measures the magnitude of the acceleration at a general level; it not only performs that activity, but it is also used as a tilt sensor, it uses gravity as a vector to establish the orientation [10]. Therefore, in the MPU these two elements are found since each one complements the other, the gyroscope detects the angle velocity in 3 directions and the accelerometer detects the angular acceleration. It is given by 3 axes, as shown in Figure 4.

At the time of programming, it became evident that the gyroscope has an orientation, so when you are at this stage you have to be careful, because if you do not program the signals to the motors are not translated correctly, instead of generating a state of balance generates the opposite effect, which the robot is not stabilized and falls.

Regarding the actuation module, it consists of 1 controller and 2 DC motors each one coupled with the wheel as shown in Figure 3. At this point when the tests were started, it was established that: first, it should be connected to direct current to be able to move the robot and second how it would be the operation with respect to the speed and torque generated, to allow it to work properly. The motors work at 12 V and a maximum speed of approximately 100 rpm.

The rotation speed of the motor output shaft is proportional to the step frequency [10], for this reason it is mentioned that a rotation speed of 100 rpm. is required to keep the robot vertical. The equation describing the wheel angle and the angular velocity of the wheel is:

$$\omega_p = \frac{d\theta}{dt} = \theta \cdot fm$$

ω_p = *Angular velocity of the wheel*
Θ = *Wheel angle*
fm = *Pulse´s frequency applied at the beginning of the cycle*

This equation depends on the design of each robot, the angle will be positive when going clockwise and negative when going counter clockwise.

Finally, the Bluetooth module is a short-range network; it is classified as an industrial standard for wireless connections. It is capable of supporting point-to-point and point-to-multipoint connections, e.g., the cell phone when connected to wireless listening devices; likewise, it is possible to establish voice and data communications [11]. It is a technology that is still widely used today, but nevertheless, with the development of new technologies it will be left behind and will no longer be so widely used.

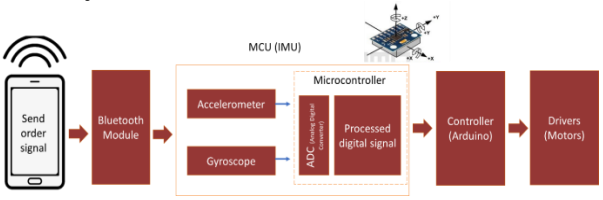

Fig. 4. Diagram of system operation.

The development of IoT (Internet of things) is a set of objects that contains integrated sensors, technologies, software, with the purpose of having a data exchange [12]; for this reason, the Wi-Fi module was developed to expand the scope of communication and in turn are connected to the internet [13], which has all the necessary components to make a fairly robust connection. Depending on the system or control element that is used (Arduino) the speed of the module is calculated, regularly between 9600 to 115200.

4. THE MATHEMATICAL MODEL

4.1 Pendulum analysis

The model describing the operation of this robot based on an inverted pendulum on a moving cart; in addition, a free body diagram is made and thus finds the equations describing the motion.

The mobile platform is its equilibrium state has a mass m at a distance L from the pivot point and a tilt angle β vertically, an acceleration of, it also experiences a force F [14]. Table 2 shows the parameters for the equations.

Figure 5, shows the inverted pendulum system, the forces in the free body diagram in the horizontal direction generate the first equation (1) and the pendulum forces in the horizontal direction generate the following equation (2).

$$P\,y + a\,y + N = F \qquad (1)$$

$$N = my + m\,c\,\beta - m\,c\,\beta^2 \sin\beta \qquad (2)$$

Table 2. Physical parameters of the inverted pendulum system

Symbol	Parameter	Units
P	Mass of car	Kg
m	Mass of pendulum	Kg
a	Friction Car	N/m*s
c	Length at pendulum center of mass	m
L	Inertia of the pendulum	kg*m^2
F	Force applied on the car force	kg*m/s^2
g	Gravity	9.8 m/s^2
N, G	Reaction forces	
y	Cart position coordinate	
β	Angle of pendulum vertically	Degrees

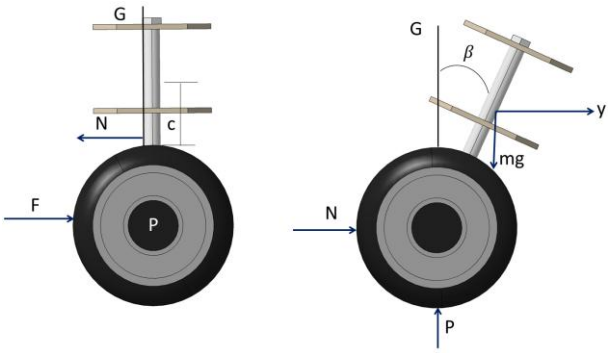

Fig. 5. Free body diagram of the inverted pendulum.

Now, substituting equation 1 into equation 2, the following equation remains:

$$(P + m)y + a\,y + m\,c\,\beta\cos\beta - m\,c\,\beta^2\sin\beta = F \quad (3)$$

Then, the sums of the forces along the axis perpendicular to the pendulum form the equation (4):

$$G\sin\beta + N\cos\beta - m\,g\sin\beta = m\,c\,\beta + my\beta\cos\beta \quad (4)$$

The summation of the moments at the centroid of the pendulum generates equation (5) and by combining (4) and (5) equation (6) is obtained.

$$-P\,j\sin\beta - N\,j\cos\beta = L\,\beta \quad (5)$$
$$(L + m\,c^2)\beta + m\,g\,c\sin\beta = -m\,c\,y\cos\beta \quad (6)$$

The equations need to be linearized in order to use linear control system techniques, based on the vertical upward equilibrium position equation, the equation is β = π [14], with a small velocity at steady state. The position deviation is represented with ∅ at steady state, where β = π + ø, is used to generate a small angle approximation in nonlinear equations, for this case:

$$\cos\beta = \cos(\pi + \emptyset) \approx -1 \quad (7)$$
$$\sin\beta = \sin(\pi + \emptyset) \approx -\emptyset \quad (8)$$
$$\beta^2 = \emptyset^2 \approx 0 \quad (9)$$

Substituting (7), (8) and (9) in (3) and (6) we obtain equations (10) and (11), noting that ***u*** is replaced by the input force *F.*

$$(L + m\,c^2)\emptyset - m\,g\,c\,\emptyset = m\,c\,y \quad (10)$$
$$(P + m)y + a\,y - m\,c\,\emptyset = e \quad (11)$$

For the generation of the transfer function, it is necessary to perform a Laplace transform under null conditions, since equations 10 and 11 are linearized, resulting in equations 12 and 13:

$$(L + m\,c^2)\,\emptyset(k)k^2 - m\,g\,c\,\emptyset(k) = m\,c\,X(k)k^2 \quad (12)$$
$$(P + m)X(k)k^2 + a\,X(k)k^2 - m\,c\,\emptyset(k)k^2 = E(k) \quad (13)$$

With the above equations it is possible to determine the output transfer ∅ and the input *E(s)*, excluding the term *X(k)* from equations 12 and 13, since these equations describe the relationship of an input and an output, then the following equation results:

$$X(k) = \left[\frac{L+mc^2}{mc} - \frac{g}{k^2}\right]\cdot\emptyset(k) \quad (14)$$

Substituting equation 14 into Equation 13 results in Equation 15

$$(M + m)\left[\frac{L + mc^2}{nc} - \frac{g}{k^2}\right]\cdot\emptyset(k)k^2 + a\left[\frac{L+mc^2}{mc} - \frac{g}{k^2}\right]\cdot\emptyset(k)k^2 - m\,c\,\emptyset(k)k^2 = E(k) \quad (15)$$

Equation 15 is left aside the terms of ∅ y *E*

$$\frac{\emptyset(k)}{E(k)} = \frac{\frac{mc}{q} * (k^2)}{k\left[k^3 + \frac{a(c + mc^2)}{q} * (k^2) - \frac{(P + m)m\,g\,c}{q} * (k) - \frac{amqc}{q}\right]} \quad (16)$$

Then, it clears that *q*

$$q = [(P + m)(L + mc^2) - (mc)^2] \quad (17)$$

In equation 16 at the origin there is a pole and a zero, so they cancel each other, and the result is:

$$P_{pendulum}(k) = \frac{\emptyset(k)}{E(k)} = \frac{\frac{mc}{q} * (k)}{k\left[k^3 + \frac{a(c + mc^2)}{q} * (k^2) - \frac{(P + m)m\,g\,c}{q} * (k) - \frac{amqc}{q}\right]}\left[\frac{rad}{N}\right] \quad (18)$$

Finally, we obtain the output and input transfer function Equation 19, eliminating $\emptyset$ of equations 12 and 13.

$$P_{pendulum}(k) = \frac{X(k)}{E(k)} = \tag{19}$$

$$= \frac{\frac{(ck^2 + mk^2c^2) - gmc}{q}}{k\left[k^3 + \frac{1}{q}(ac + amc^2 * (k^2) - (P + m)m\,g\,c * (k) - amqc)\right]} \left[\frac{rad}{N}\right]$$

It is necessary to generate a model of states that are represented by equations 18 and 19 in matrix form, since these two functions are linear and became first order differential equations, in addition, the position of the cart and the pendulum are part of the output so the matrix has 2 rows:

$$\begin{bmatrix} \dot{y} \\ \ddot{y} \\ \dot{\beta} \\ \ddot{\beta} \end{bmatrix} = \begin{bmatrix} 0 & 1 & 0 & 0 \\ 0 & \frac{-(L+mc^2)a}{L(P+m)+Pmc^2} & \frac{m^2gc^2}{L(P+m)+Pmc^2} & 0 \\ 0 & 0 & 0 & 1 \\ 0 & \frac{-mca}{L(P+m)+Pmc^2} & \frac{mgc(P+m)}{L(P+m)+Pmc^2} & 0 \end{bmatrix} \begin{bmatrix} y \\ \dot{y} \\ \beta \\ \dot{\beta} \end{bmatrix} + \begin{bmatrix} 0 \\ \frac{L+mc^2}{L(P+m)+Pmc^2} \\ \beta \\ \frac{mc}{L(P+m)+Pmc^2} \end{bmatrix} * E \tag{20}$$

$$y = \begin{bmatrix} 1 & 0 & 0 & 0 \\ 0 & 0 & 1 & 0 \end{bmatrix} \begin{bmatrix} y \\ \dot{y} \\ \beta \\ \dot{\beta} \end{bmatrix} + \begin{bmatrix} 0 \\ 0 \end{bmatrix} e \tag{21}$$

The mathematical analysis found above is replaced in the equations found with the corresponding values for the robot presented in table 3.

Table 3. Physical parameters calculated

Symbol	Name	Parameter	Units
P	*Mass of car*	*0.8*	*Kg*
m	*Mass of pendulum*	*0.7*	*Kg*
a	*Friction Car*	*0.1*	*N/m*s*
c	*Length at pendulum center of mass*	*0.05*	*m*
L	*Inertia of the pendulum*	*0.04*	*kg*m²*
g	*Gravity*	*9.8*	*m/s²*

Substitute in equations 18 and 19

$$P_{pendulum}(k) = \frac{\emptyset(k)}{E(k)} = \tag{22}$$

$$= \frac{0.072k}{k\left[k^3 + 0.072k^2 - 8.87k - 3.5x10^{-3}\right]} \left[\frac{rad}{N}\right]$$

$$P_{pendulum}(k) = \frac{X(k)}{E(k)} = \tag{23}$$

$$\frac{\frac{(0.05k^2 + 1.75x10^{-3}k^2) - 0.343}{0.058}}{k\left[k^3 + \frac{1}{q}(0.005 + 1.75x10^{-3}k^2 - 0.5145k - 2.03x10^{-4})\right]} \left[\frac{rad}{N}\right]$$

Finally, there are some considerations, the system will always start in an equilibrium state and the initial conditions will be 0, the pendulum will have an error of a few degrees of tolerance, thus satisfying the linear model [1] and when the robot has been connected its equilibrium state will start in a staggered way (displacement of the pendulum θ).

4.2 Analysis of DC motors and parameters

The robot works with direct current; therefore, a rotary motion is generated which is coupled to the wheels, this produces translational motion [1]. Figure 6 shows the free body diagram of the motor operation, the energy input of the motors is proportional to the induced current and the intensity of the magnetic field; also, the motors contain magnets that allow to establish that they have a constant magnetic field, for this reason the motor is proportional to the induced current by the factor Kt[1]. Some physics' motor parameters are listening in table 4.

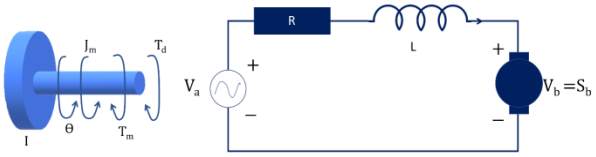

Fig. 6. Free body diagram of DC motors.

Table 4. Parameters of motors

Symbol	Parameter	Units
I	*Moment of Inertia*	*0.01944 Kg*m²*
b	*Viscous friction constant of the motor*	*0.1 N*m*s*
S	*Motor torque constant and back - phase constant*	*0.2*
R	*Electrical resistance*	*3.33 Ω*
L	*Electrical inductance*	*0.002 Wb/A = 0.002 H*

$$T = S_t i \tag{24}$$
$$e = S_t \beta \tag{25}$$
$$S_e = S_t \tag{26}$$

In equation 26 represents the motor constant and the automotive force.

$$I\ddot{\beta} + b\dot{\beta} = si \tag{27}$$
$$L\frac{di}{dt} + Ri = V - S\dot{\theta} \tag{28}$$

A Laplace transform is performed with equations 13 and 14:

$$k(J\,k + b)\dot{\beta}(k) = g\,L(k) \tag{29}$$
$$k(L\,k + R)\,L(k) = V(k) - G\,k\,\dot{\beta}(k) \tag{30}$$
$$\frac{\dot{\beta}(k)}{V(k)} = \frac{S}{(I\,k + b)(Lk + R) + S^2} \tag{31}$$

The relation between torque vs. input voltage

$$\frac{T(k)}{V(k)} = \frac{S(k + I\,b)}{(k\,L + R)(k\,I + b) + S^2} \tag{32}$$

At the end, to find the transfer equation we substitute in equations 31 and 32, in the first equation we take the velocity with input voltage and the other is the same with input voltage.

$$H(k) = \frac{\dot{\beta}(k)}{V(k)} = \frac{0.2}{0.647552k+0.3733} \quad (33)$$

$$P(k) = \frac{T(k)}{V(k)} = \frac{0.2 + 0.0000194}{0.064935k+0.3733} \quad (34)$$

The behaviour of the DC motors that have the self-balancing robot in figure 7; where the values of electrical resistance and inductance are involved, equations 33 and 34 were entered into the program that graphs the behaviour. The red line corresponds to equation 33 and the blue line to equation 34.

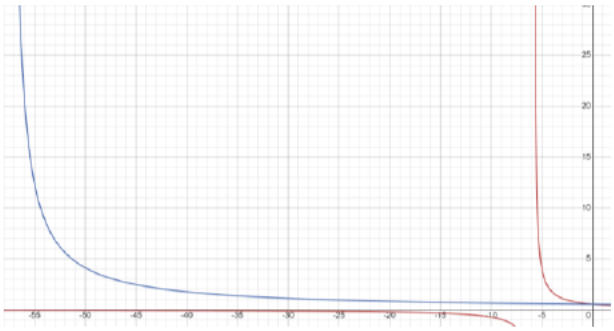

Fig. 7. Graphic results of DC motor performance.

4.3 Controller analysis

The PID control (Proportional, Integral and Derivative) is a controller that aims to establish the error in steady state, using as reference the input signals; in addition, it is possible to know how its state will be in the future, through a derivative function that predicts the output of the process. Block diagram is showing in figure 8. Currently, they are widely used in industries to control different industrial processes, to control and predict the processes of the companies, likewise, every day they are evolving to go according to the developed technology [15]. The operation with respect to the self-balancing robot, where the voltage signal is taken as input and motor speed as output.

The PID controller parameters and its respond are presented in figure 8 and 9; it has 3 well know variables: proportional control (Kp), proportional control (Kd) and integral control action (Ki). According to the controller design the input to the controller is fed back to the system error signal given by nTm; similarly, the error deviation between the desired state of the tilt angle αB=0 and the real time angle measured by the robot IMU, then the signals enter these 3 states simultaneously and are fed back in the same way. One factor that allows reducing the angular position error is the proportional control Kp, which allows the motors to move and rotate in the same direction to which the signals are being sent [16].

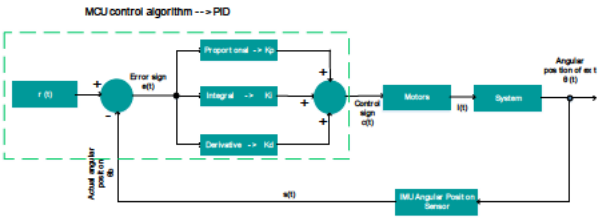

Fig. 8. Representation of PID controller operation.

In figure 9 is showing the PID controller parameters for the self-balancing robot with a constants of: Kp: 60; Kd: 2.2-3.5; Kd: 250.

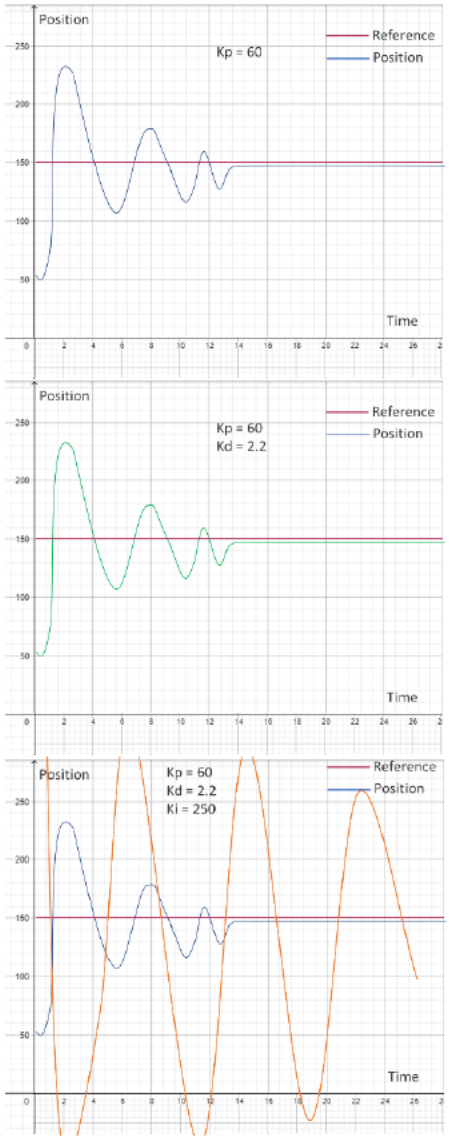

Fig. 9. Graphic of PID simulations and results

5. MOTION ANALYSIS

To perform the motion analysis, a function was implemented in the code to retrieve data from the MPU6050 sensor such as the degree of inclination, linear acceleration and angular velocity decomposed for the 3 axes and contrasts them over time in order to observe the relationship between the variables.

Table 5. Data collection for acceleration, velocity, and grade of inclination.

	Aceleration			Velocity			Inclination angle
Seconds	X	Y	Z	X	Y	Z	°
0,186	-0,03	-0,17	1,04	0,186	0,79	0,44	87,57
0,372	-0,06	0,16	1,05	0,372	0,5	0,34	83,66
0,558	-0,05	0	1,08	0,558	-3,37	0,27	82,11
0,744	-0,06	0,01	1,08	0,744	-0,74	-0,56	82,48
0,93	-0,05	0,19	1,07	0,93	5,16	0,53	84,8
1,116	0	0,27	1,08	1,116	-3,8	0,39	86,55
1,302	-0,09	0	1,09	1,302	1,44	1,4	82,34
1,488	-0,06	0,04	1,07	1,488	-4,77	0,19	86,49
1,674	-0,06	-0,14	1,08	1,674	1,4	1,5	85,57
1,86	-0,07	0,06	1,09	1,86	6,24	0,86	88,07
2,046	-0,04	0,11	1,05	2,046	-1,56	-0,27	84,16
2,232	0,12	-0,48	1,26	2,232	-1,84	0,42	88,26
2,418	-0,03	0,03	1,03	2,418	5,92	0,63	85,62

Once obtained and recorded the values in table 5, we proceed to contrast the variables by plotting the variation in acceleration in the 3 axes over time obtaining the graph represented in Figure 10

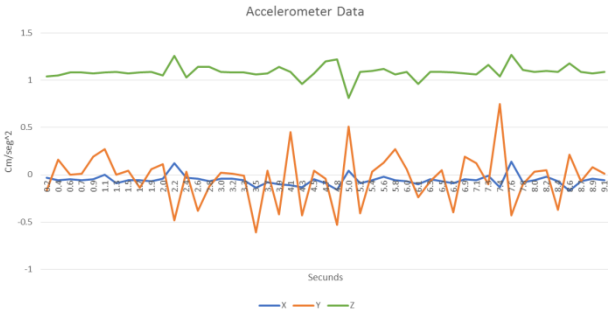

Fig. 10. Graphic results of acceleration versus time

Having said this, it can be observed in figure 10 that in the first instants of the movement the acceleration values are close to zero, indicating that the robot is starting from the equilibrium phase of the same, once it begins its forward movement it is observed as there is a considerable variation in the acceleration of the X axis where it is corroborated that the value and the sign indicates where and how intense is the movement, on the other hand it can be observed that when the movement begins, the graph begins to oscillate and the lines try to synchronize in the phases for the three axes indicating that the system is looking for "self-balancing".

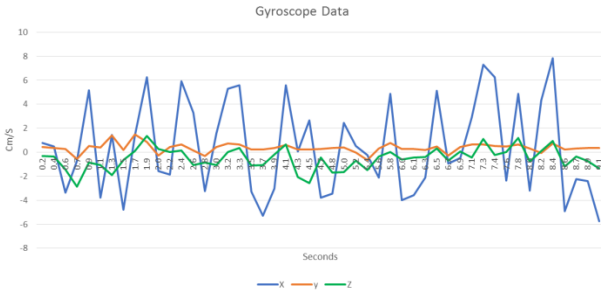

Fig. 11. Graphic results of velocity versus time

Likewise, we repeat the procedure previously mentioned for the case of the linear velocity obtaining the graph shown in figure 11.

With the graph, it can be stated that initially the linear velocity in the X axis is positive and increases reflecting the forward motion, then as the robot moves forward this value decreases considerably compared to the initial speed, so it is balancing seeking to counteract the angle of inclination to the point that the coefficient is negative to regain its balance.

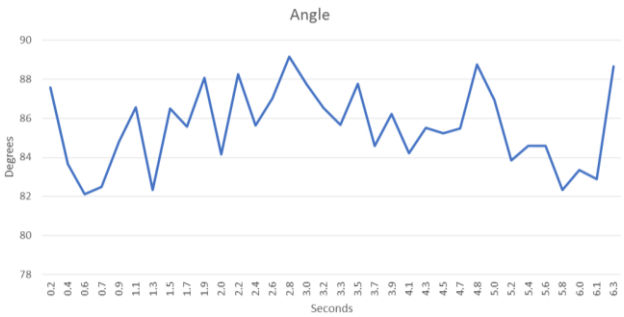

Fig. 12. Graphic results of grade of inclination vs time

Finally, the angle of inclination is graphed in Figure 12, for the movement, where it was obtained that the angle at the beginning is positive and as time passes it gradually decreases to values close to zero, similar to the relationship with the speed.

6. RESULTS AND DISCUSSION

The implementation of the inverted pendulum theory is a process that takes several days of research and implementation. The first phase is to assemble and hold all the electronic components on top of the robot, this also helps to generate a balance in the weight of the robot. The second phase is to test the IMU sensor, which is the most important component of this type of Segway robot.

The robot works with continuous source, therefore when it was connected to the current the first reaction was to perform many involuntary movements, in the first test performed the degrees of tolerance in which the robot was going to oscillate forward and backward were chosen based on the parameters of the robot, however, in this test allowed adjusting the degrees of equilibrium. Additionally, all the mathematical and physical support of the robot was tested, with all the parameters corresponding to the robot, as shown in figure 7, the motors have a normal behaviour when the robot is in operation, although in the curves it is expected that the two lines are closer. However, the motors work correctly.

In the robot code it was established that the state of equilibrium is 180°, based on the tests carried out it was determined that for the robot to go forward an extra 1° must be added, that is, 181°; likewise, to go backwards it is 179°. Likewise, any rough movement in the robot generates a small deviation in the order signals to the robot; therefore the elements must be well secured in the robot, as shown in figure 13.

Fig. 13 . Movements of the self-balancing robot

7. CONCLUSIONS

The purpose of this article is to show the design and functionality of the dual-wheeled robot model, starting by explaining the mechanical design, the material model and the results obtained in the development of the project. Segway robots play a vital role nowadays due to their wide variety of uses and purposes, as it is now being used as a means of transportation, due to its design, speed and ergonomics; besides, compared to other means of transportation, it occupies little space and it is affordable for all people.

In conclusion, an algorithm was developed and implemented by means of an Arduino code that allows to keep the robot in balance from its initial phase when it is connected to direct current until when any movement is generated, that is to say, it remains stable throughout the entire route. Also, after the tests performed (figure 10) the robot is resistant to external disturbances or small shocks that may have and that generate alterations in it sent signals.

At long last, the IMU sensor that brings integrated accelerometer and gyroscope is important to know well the direction and sense that can bring, so program it properly in the code, because otherwise the robot will not find any direction to which it should move.

REFERENCES

[1] Junoh, S. A. (2015). *Two-wheeled balancing robot controller designed using pid* (Doctoral dissertation, Universiti Tun Hussein Onn Malaysia).

[2] Browning, B., Searock, J., Rybski, P. E., & Veloso, M. (2005). *Turning segways into soccer robots. Industrial Robot*: An International Journal, 32(2), 149-156.

[3] Pinto, L. J., Kim, D.-H., Lee, J. Y., & Han, C.-S. (2012). *Development of a Segway robot for an intelligent transport system*. 2012 IEEE/SICE International Symposium on System Integration (SII). doi:10.1109/sii.2012.6427308

[4] Klomp, S. (2022). *Transportation of Injured Athletes* (Bachelor's thesis, University of Twente).

[5] Abdullah M. Almeshal; *"Dynamic modeling and control of a two-wheeled robotic machine with an extended rod"*. (2011) Doctorate thesis. University of Sheffield, UK.

[6] Gong, Y., Hartley, R., Da, X., Hereid, A., Harib, O., Huang, J. K., & Grizzle, J. (2019, July). *Feedback control of a cassie bipedal robot: Walking, standing, and riding a segway.* In 2019 American Control Conference (ACC) (pp. 4559-4566). IEEE.

[7] Raviv, D., & Barb, D. (2019, June). *A Visual, Intuitive and Engaging Approach to Explaining the Center of Gravity Concept in Statics*. In Proceedings of the 2019 126th ASEE Annual Conference & Exposition, Tampa, FL, USA (pp. 15-19).

[8] RUAN, X., & ZHAO, J. (2010). *Flexible Two-wheeled Self-balancing Robot Control Based on Hopfield Neural Network*. ROBOT, 32(3), 405–413.

[9] Vilanova, R., & Alfaro, V. M. (2011). *Robust PID Control: A Panoramic View*. Ibero-American Journal of Automation and Industrial Informatics RIAI, 8 (3), 141-158.

[10] Nilsson, J. O., & Skog, I. (2016, May). *Inertial sensor arrays—A literature review*. In 2016 European Navigation Conference (ENC) (pp. 1-10). IEEE.

[11] ElGibreen, H.; Al Ali, G.; AlMegren, R.; AlEid, R.; AlQahtani, S. Telepresence *Robot System for People with Speech or Mobility Disabilities. Sensors* 2022, 22, 8746. https://doi.org/10.3390/s22228746

[12] Gong, W. (2016). *The Internet of Things (IoT): What is the potential of the internet of things (IoT) as a marketing tool?* (Bachelor's thesis, University of Twente).

[13] Wenbo, Y., Quanyu, W., & Zhenwei, G. (2015, July). *Smart home implementation based on Internet and WiFi technology*. In 2015 34th Chinese Control Conference (CCC) (pp. 9072-9077). IEEE.

[14] Azar, A. T., Ammar, H. H., Barakat, M. H., Saleh, M. A., & Abdelwahed, M. A. (2018, September). *Self-balancing robot modeling and control using two degree of freedom PID controller*. In International Conference on Advanced Intelligent Systems and Informatics (pp. 64-76). Springer, Cham.

[15] Díaz-Rodríguez, I. D., Han, S., & Bhattacharyya, S. P. (2019). *Analytical design of PID controllers*. Springer International Publishing.

[16]Jiménez, F. R. L., Ruge, I. A. R., & Jiménez, A. F. L. (2020). *Modeling and control of a two wheeled auto-balancing robot: A didactic platform for control engineering education*. In Proceedings of the LACCEI international Multi-conference for Engineering, Education and Technology. Latin American and Caribbean Consortium of Engineering Institutions. https://doi.org/10.18687/LACCEI2020.1.1.556

[17]Watson, M. T., Gladwin, D. T., Prescott, T. J., & Conran, S. O. (2019, May). *Velocity constrained trajectory generation for a collinear Mecanum wheeled robot*. In 2019 International Conference on Robotics and Automation (ICRA) (pp. 4444-4450). IEEE.

[18]Bhatti, O. S., Rizwan, M., Shiokolas, P. S., & Ali, B. (2019). *Genetically optimized ANFIS-based PID controller design for posture-stabilization of self-balancing-robots under depleting battery conditions*. Journal of Control Engineering and Applied Informatics, 21(4), 22-33.

[19]Wang, C., Yin, G., Liu, C., & Fu, W. (2016, June). *Design and simulation of inverted pendulum system based on the fractional PID controller*. In 2016 IEEE 11th Conference on Industrial Electronics and Applications (ICIEA) (pp. 1760-1764). IEEE.

[20]LIU, Shuaishuai, et al. *Research on wheel-legged robot based on LQR and ADRC*; 2022.

[21]KANG, Peng; MENG, Haibin; XU, Wenfu. *A unified modeling and trajectory planning method based on system manipulability for the operation process of the legged locomotion manipulation system*. Robotica, 2023, p. 1-16.

[22]CH, Ronal P., et al. *Acceleration Feedback Controller Processor Design of a Segway*. En 2022 IEEE 7th Southern Power Electronics Conference (SPEC). IEEE, 2022. p. 1-6.

[23]Tang, H., Zhang, J. W., Pan, L., and Zhang, D. (January 10, 2023). "*Optimum Design for a New Reconfigurable Two-Wheeled Self-Balancing Robot Based on Virtual Equivalent Parallel Mechanism*." ASME. J. Mech. Des. May 2023; 145(5): 053302. https://doi.org/10.1115/1.4056575